



# 1 21<sup>st</sup> Century Asian air pollution impacts glacier in northwestern 2 Tibet

3 M. Roxana Sierra-Hernández<sup>1</sup>, Emilie Beaudon<sup>1</sup>, Paolo Gabrielli<sup>1,2</sup>, and Lonnie G. Thompson<sup>1,2</sup>

4  
5 <sup>1</sup>Byrd Polar and Climate Research Center, The Ohio State University, Columbus, OH, 43210, USA

6 <sup>2</sup>School of Earth Sciences, The Ohio State University, Columbus, OH, 43210, USA

7 *Correspondence to:* M. Roxana Sierra-Hernández (sierra-hernandez.1@osu.edu)

8

9 **Abstract.** Over the last four decades, Asian countries have undergone significant economic development leading to  
10 rapid urbanization and industrialization in the region. Consequently, fossil fuel consumption has risen dramatically  
11 worsening the air quality in Asia. Fossil fuel combustion emits particulate matter containing toxic metals that can  
12 adversely affect living organisms, including humans. Thus, it is imperative to investigate the temporal and spatial  
13 extent of metal pollution in Asia. Recently, we reported a continuous and high-resolution 1650–1991 ice core record  
14 from the Guliya ice cap in northwestern Tibet, China showing a contamination of Cd, Pb and Zn during the 20<sup>th</sup>  
15 century. Here, we present a new continuous and high-resolution ice core record of trace metals from the Guliya ice  
16 cap that comprises the years between 1971 and 2015, extending the 1650–1991 ice core record into the 21<sup>st</sup> century.  
17 Non-crustal Cd, Pb, Zn and Ni enrichments increased since the 1990s reaching a maximum in 2008. The enrichments  
18 of Cd, Pb, Zn, and Ni increased by ~75 %, 35 %, 30 %, and 10 %, respectively during the 2000–2015 period relative  
19 to 1971–1990. Our analysis suggests that emissions from Pakistan’s fossil fuel combustion (by road transportation  
20 and the manufacturing and construction industries) became the dominant source of Cd, Pb, Zn, and Ni deposited on  
21 Guliya between 1995 and 2015. However, it is possible that emissions from Central Asia, Afghanistan, India, Nepal,  
22 and the Xinjiang province in China have also impacted Guliya during the 21<sup>st</sup> century. The enrichments of Cd, Zn,  
23 and Ni declined after 2008 likely due to a coal consumption decrease in Pakistan at that time. This new record  
24 demonstrates that the current emissions in Asia are impacting remote high-altitude glaciers in the region and that  
25 mitigation policies and technologies should be enforced to improve the air quality as economic development continues  
26 in most Asian countries.

## 27 1 Introduction

28 Atmospheric trace elements (TE), including toxic metals (e.g., Hg, Pb, Cd) have dramatically increased since the 19<sup>th</sup>  
29 century due to human activities (Pacyna and Pacyna, 2001; Tian et al., 2015). Some TEs are highly toxic and harmful  
30 to an array of animals, plants and humans. Atmospheric TEs can originate from natural sources/processes in the  
31 environment such as windborne dust, wildfires, sea-spray aerosols, volcanic activity, and from vegetation (Nriagu,  
32 1989a, b). TEs are also released into the atmosphere by human activities including: 1) the combustion of fossil fuels  
33 including coal, oil and its distillates (e.g., gasoline, jet fuel, diesel); 2) industrial processes such as mineral, and metal



34 production; 3) agriculture practices that include the use of fertilizers and pesticides; and 4) waste disposal (Pacyna  
35 and Pacyna, 2001).

36 Various anthropogenic sources, including fossil fuel combustion and smelting, emit fine ( $< 2.5 \mu\text{m}$ ) particulate matter  
37 ( $\text{PM}_{2.5}$ ) which can contain toxic metals such as As, Cd, Pb, and Zn. Due to its small size, the lifetime of  $\text{PM}_{2.5}$  in the  
38 atmosphere can last for over a week, thereby allowing it to be transported and deposited far from its initial sources  
39 (e.g., onto remote glaciers) (Pacyna and Pacyna, 2001; Marx and McGowan, 2010).

40 Since the 1980s, Asian countries such as China, India, Pakistan, Nepal, Bangladesh and others have undergone  
41 significant and rapid economic growth, leading to considerable urbanization and industrialization in the region.  
42 Consequently, fossil fuel combustion has risen dramatically in most of these countries worsening the air quality. In  
43 particular, China and India, the second and fifth largest economies in the world according to the International Monetary  
44 Fund, are respectively the largest and third largest emitters of both  $\text{CO}_2$  and  $\text{PM}_{2.5}$ .

45 The rapid economic growth of China has been the result of its economic reform and open policy beginning in 1978  
46 after Mao Zedong's death and the subsequent five-year plans (FYP) implemented by the Chinese government. With  
47 their economic growth, China and India started to increase their coal consumption since ~1970 amplifying the global  
48 atmospheric emissions of  $\text{CO}_2$  and  $\text{PM}_{2.5}$  (Crippa et al., 2018; EDGARv4.3.2, 2017).

49 In 1999, the Chinese government implemented the "Western Development" policy in the 10<sup>th</sup> FYP to improve the  
50 quality of the environment in the east and to transfer energy (West to East energy program) and mineral resources  
51 from the west to the rest of the country (Chen et al., 2010; Lai, 2002; Dong and Yang, 2014). For this purpose, the  
52 necessary infrastructure (e.g., airports, railways, highways, water infrastructure, power lines) was built. As a result,  
53 energy consumption (Jianxin, 2016) and atmospheric emissions (Liu et al., 2015) have been increasing significantly  
54 in western China.

55 In particular, the Xinjiang Uygur Autonomous Region, situated in an arid region of Northwestern China, has become  
56 important for the Western Development implementation because of its location on the new Silk Road and its large  
57 reserves of oil, gas, and coal (Fridley et al., 2017; Chen et al., 2010; Dong and Yang, 2014). Three mountain ranges  
58 shape the topography of this province: the Altai on the northern border, Tien Shan in the center, and the western  
59 Kunlun Mountains, where the Guliya ice cap is located (see below), along the southern border with Tibet (Fig. 1a).

60 Pakistan, to the southeast of Xinjiang, gained its independence in 1947 after which its population rose very rapidly  
61 becoming the world's sixth most populated country by 2003 (UN, 2017). Although Pakistan's economic growth has  
62 been much lower than China's and India's, urban Pakistani cities are among the most polluted in the world (WHO,  
63 2016) due to the high population growth, industrialization and a significant increase of motor vehicles that lack  
64 emission controls and use low quality gasoline/diesel. The number of registered vehicles increased by ~400 % between  
65 1996 (3.838 million) and 2014 (15.168 million) (Bajwa, 2015). Emissions from motor vehicles (60–70 %), industry,  
66 and the generation of ~54,000 t of solid waste per day which is either dumped or incinerated have been estimated as  
67 the principal sources of  $\text{PM}_{2.5}$  and air pollution in Pakistan (Colbeck et al., 2010; Sánchez-Triana et al., 2014).



68 For the year 1995, Pacyna and Pacyna (2001) estimated that non-ferrous metal production was the largest source of  
69 As, Cd, Cu, In, and Zn; while coal combustion was the major source of Cr, Hg, Mn, Sb, Se, Sn, and Tl, and oil  
70 combustion was the major source of Ni and V, both worldwide and in Asia. For the same year, these authors estimated  
71 that leaded gasoline was the major source of Pb worldwide as well as in Asia. However, changes in emissions of  
72 atmospheric TEs have occurred during the 21<sup>st</sup> century in Asia due to the following: 1) China and India emerged as  
73 the fastest growing economies and most populated countries in the world (UN, 2017); 2) developing countries such  
74 as Pakistan, Nepal and Bangladesh have significantly increased their national economic activities since the 1980s–  
75 1990s; 3) temporal and regional variations in the implementation of control emission technologies and air quality  
76 standards (often higher concentrations than those recommended by the World Health Organization); 4) leaded gasoline  
77 was banned in 2000 in China, India, and Nepal and in 2002 in Pakistan, while it is still consumed in Afghanistan.  
78 Therefore, it is imperative to study the spatial and temporal effects of these new pollution sources and their resulting  
79 impacts on the environment.

80 Atmospheric emissions estimates are associated with large uncertainties due to inaccurate statistical information, the  
81 lack of field data and limited temporal and spatial coverage of observations. Thus, natural registers of past  
82 environmental conditions such as glaciers, which are influenced only by deposition of atmospheric species, are  
83 essential for reconstructing time series of atmospheric metal depositions (Hansson et al., 2015; Cooke and Bindler,  
84 2015; Gabrielli and Vallelonga, 2015; Marx et al., 2016) that can be further used by modelers to reconstruct past  
85 emissions and project future atmospheric contamination trends.

86 Recently, we obtained a 350-year (1650–1991) high-resolution TE record (Sierra-Hernández et al., 2018) using an ice  
87 core drilled in 1992 from the Guliya ice cap located in northwestern China, specifically in Tibet’s Kunlun Mountains  
88 (35° 17.37’ N; 81° 29.73’ E; 6200 m a.s.l.) (Thompson et al., 1995) (Fig. 1a). Outside of the Arctic and Antarctica,  
89 the glaciers in the Kunlun Mountains, along with those in Tibet and the Himalayas, are the largest reservoir of ice on  
90 the globe and are commonly referred to as the “Third Pole”. This glacial region is the source for numerous rivers in  
91 Asia which provide water to hundreds of millions of people. The 1992 Guliya TEs record showed that long-distance  
92 emissions from coal combustion in Europe were likely deposited on the ice cap between 1850 and 1940 (Sierra-  
93 Hernández et al., 2018). Additionally, Pb, Cd, and Sn enrichments were detected between 1975 and 1991. The origin  
94 of these more recent enrichments could not be determined as more anthropogenic sources have emerged, especially  
95 in this region.

96 Here, we use a new ice core retrieved from Guliya in 2015 to extend the 1650–1991 TEs record into the 21<sup>st</sup> century  
97 (1971–2015) and to determine the impacts of the recent emission changes in Asia on the western Kunlun Mountains  
98 glaciers. This study fills a temporal and spatial gap in the investigation of atmospheric toxic trace metals in  
99 Northwestern China where atmospheric emission data are limited.



## 100 2 Methodology

### 101 2.1 Guliya cores

102 In 2015, two ice cores (309.73 m and 72.40 m long) were extracted from the plateau of the Guliya ice cap (6200 m  
103 a.s.l), in close proximity to the 1992 drilling site. The timescale was constructed by annual layer counting using three  
104 fixed horizons at 2015 (surface of the glacier), at 1992 corresponding to the surface of the 1992 core (at 6 m in the  
105 shallow core), and at 1963 (at 10.9 m in the shallow core determined by beta radioactivity from the Arctic  
106 thermonuclear tests). Annual layers were determined using both cores by matching the signals of at least three different  
107 parameters ( $\text{Cl}^-$  and  $\text{Na}^+$ , dust and  $\text{Ca}^{2+}$ ,  $\text{SO}_4^{2-}$ , and  $\delta^{18}\text{O}$ ). Dating uncertainties are estimated at 1–2 years between the  
108 fixed points and may be the result of the very low annual accumulation (~230 mm water equivalent) and surface-  
109 alteration processes such as snow redistribution through wind. Details of the drilling operation, the ice cores, and the  
110 timescale can be found in Thompson et al. (2018).

### 111 2.2 Sample preparation and ICP-SFMS analysis

112 The preparation of the samples and their analysis were performed following the same procedures adopted for the 1992  
113 Guliya core samples (Sierra-Hernández et al., 2018). Briefly, 159 ice samples comprising the years 1971 (11 m) to  
114 2015 (0.06 m) were cut from the 309.73 m long-deep ice core. To ensure the analysis of 3–4 samples year<sup>-1</sup>, the sample  
115 resolution was adjusted between 4.5 and 11 cm accordingly. The samples were rinsed three times with nanopure water  
116 (18.3 MΩ) in a class-100 cleanroom and placed in acid pre-cleaned LDPE containers (Nalgene) to melt. Once melted,  
117 samples were transferred into acid pre-cleaned LDPE vials where nitric acid ( $\text{HNO}_3$ , Optima for Ultra Trace Element  
118 Analysis, Fisher Scientific) was added to obtain a 2 % (v/v) acidified sample. The samples were then stored in the  
119 cleanroom for a 30-day period during which the acid leaching process took place. At the end of the 30-day period, the  
120 samples were immediately analyzed or stored at  $-32\text{ }^\circ\text{C}$ .

121 Twenty-nine TEs (Ag, Al, As, Ba, Bi, Cd, Co, Cr, Cs, Cu, Fe, Ga, Li, Mg, Mn, Mo, Na, Nb, Ni, Pb, Rb, Sb, Sn, Sr,  
122 Ti, Tl, U, V, and Zn) were measured in the samples by Inductively Coupled Plasma Sector Field Mass Spectrometry  
123 (ICP-SFMS) (Element 2) (Sierra-Hernández et al., 2018; Beaudon et al., 2017). Trace elements were quantified using  
124 linear calibration curves constructed from external standards analyzed before and after the samples.

125 Detection limits, procedural blanks, and accuracy results are presented in Table S1. Detection limits correspond to  
126 three standard deviations of the concentration of 10 blank measurements (2 % optima  $\text{HNO}_3$  aqueous solution) and  
127 fluctuate between  $0.01\text{ pg g}^{-1}$  for Bi to  $0.2\text{ ng g}^{-1}$  for Fe and  $0.4\text{ ng g}^{-1}$  for Na (Sierra-Hernández et al., 2018; Beaudon  
128 et al., 2017). To verify that the sampling and decontamination procedures did not add TEs to the ice core samples,  
129 procedural blanks were made with nanopure water and analyzed with the ice core samples (Uglietti et al., 2014). Their  
130 TE concentrations are considered negligible for all TEs, apart from Nb (9 %), as they were lower than 2 % of the  
131 corresponding median concentration. The accuracy of the ICP-SFMS was determined each day of analysis using a 20-  
132 fold dilution of a TMRain-95 certified solution (Environment Canada). The obtained TE concentrations fell within  
133 the uncertainty limits in the certificate of analysis.



### 134 2.3 Non-crustal contribution

135 Enrichment Factor (EF) and Excess concentrations are used to assess the crustal and non-crustal (e.g., anthropogenic)  
136 origins of each TE.

137 The EF is obtained following Eq. (1)

$$138 \quad EF = [TE / Fe]_{ice} / [TE / Fe]_{PSA} \quad (1)$$

139 where  $[TE / Fe]_{ice}$  corresponds to the ratio of a particular TE concentration to that of Fe in an ice sample and  
140  $[TE / Fe]_{PSA}$  is the respective ratio in dust samples used as potential source area (PSA). For details about the Guliya  
141 PSA and EFs derived from PSAs, the reader is referred to Sierra-Hernández (2018).

142 Similar to the previous Guliya TEs study, Fe was chosen as the crustal reference due to its stability and high abundance  
143 in soil and rocks (Wedepohl, 1995), its high concentration both in the ice core samples and the PSAs; and the ability  
144 of the ICP-SFMS to measure Fe with high accuracy and precision (Uglietti et al., 2014).

145 Excess concentrations are calculated following Eq. (2)

$$146 \quad Excess = [TE]_{ice} - ([TE/Fe]_{pre-industrial} \times [Fe]_{ice}) \quad (2)$$

147  $[TE]_{ice}$  and  $[Fe]_{ice}$  are the concentrations of a particular TE and of Fe in the sample;  $[TE/Fe]_{pre-industrial}$  is the median of  
148 the TE concentration to the Fe concentration during the pre-industrial period (1650-1750), as obtained from the 1992  
149 Guliya record (Sierra-Hernández et al., 2018).

150 To be consistent with our previous Guliya TEs publication, a TE will be considered of non-crustal origin (enriched)  
151 when increases in EF and Excess concentration are significantly different from its background (pre-industrial levels),  
152 using both a two-sample t-test for averages and the Mann–Whitney test for medians ( $p < 0.01$ ).

### 153 2.4 Statistical analysis

154 All statistical analyses, factor analysis, cluster analysis, Mann–Whitney test for medians and a two-sample t-test for  
155 averages and Mann–Kendall trend tests, were performed using Minitab 17 and 18. The Mann–Whitney test and the  
156 two-sample t-test were applied to the entire data set subdivided into three groups: 1971–1990, 1990–2000, and 2000–  
157 2015.

## 158 3 Results and discussion

159 The time series of Cd, Pb, Zn, Ni, and Al concentrations, Excess concentrations and EFs are presented as 5-year  
160 running means in Fig. 2. The concentrations show high variability between 1971 and 1990 that decreases after 1990  
161 perhaps as a result of the decreasing frequency of dust storms in the region (Thompson et al., 2018).



162 The Excess concentrations and EFs of Cd, Ni, Pb, and Zn increase after ~1990 and continue to increase more rapidly  
163 and significantly after 2000. Their EF averages increase by ~10 % during 1990–2000, and during 2000–2015 by 75  
164 % (Cd), 35 % (Pb), 30 % (Zn) and 10 % relative to the 1971–1990 period.

165 A comparison between the 1992 and the 2015 Guliya TE records is discussed in the Supplement (Fig. S1). The 1992  
166 Guliya TE records show that enrichments of Pb and Cd begin ~1975 while the 2015 Guliya record shows they continue  
167 to rise into the 21<sup>st</sup> century until ~2008 when the Cd enrichment started to decrease. In addition to these TEs, the 2015  
168 record exhibits clear increases in Zn and Ni EFs since the 1990s into the 21<sup>st</sup> century, and similar to Cd, they decrease  
169 after 2008. The Zn enrichment began to increase after 1975 similar to Pb and Cd; however, the signal may have been  
170 overwhelmed by its crustal component in the 1992 core record rendering it undetectable.

171 A factor analysis method was used to assess the shared variability among TEs to determine possible common sources  
172 (Sierra-Hernández et al., 2018). Much of the variance (94%) is explained by both Factor 1 (73 %) and Factor 2 (21  
173 %) (Table S2). Similar to the 1992 TE results, TEs of crustal origin (e.g., Al, As, Ba, Fe, Mg, Mn, Ti, and V) fall into  
174 Factor 1. In Fig. S2 the time series of Factor 1 scores are compared with the ice core concentrations of dust particles  
175 ( $\rho = 0.20$ ,  $p = 0.2$ ) and with the typical crustal TEs Fe and Al. Water-soluble TEs (e.g., Na, Sr), which are deposited  
176 in the form of salts (evaporites) or carbonates, contribute to Factor 2 (Sierra-Hernández et al., 2018) (Table S2). This  
177 is shown in the Factor 2 time series (Fig. S3) which have significant ( $p < 0.001$ ) correlations with the ions  $\text{Cl}^-$  ( $\rho =$   
178  $0.83$ ),  $\text{NO}_3^-$  ( $\rho = 0.84$ ),  $\text{SO}_4^{2-}$  ( $\rho = 0.90$ ),  $\text{Na}^+$  ( $\rho = 0.92$ ),  $\text{NH}_4^+$  ( $\rho = 0.62$ ),  $\text{K}^+$  ( $\rho = 0.84$ ),  $\text{Mg}^{2+}$  ( $\rho = 0.86$ ), and  $\text{Ca}^{2+}$  ( $\rho$   
179  $= 0.75$ ) (Thompson et al., 2018).

180 Factor 3 explains 2 % of the variance and is loaded in Cd, and to a lesser extent in Bi, Cu, Mn, Ni, Pb, Sn, Tl, and Zn.  
181 Although 2 % represents a low variance possibly within the background noise, it could still have a physical  
182 significance (Moore and Grinstead, 2009). In order to determine if Factor 3 is physically explainable, its time series  
183 scores are plotted with the EFs of Cd, Pb and Zn in Fig. 3.

184 Factor 3 was found to be significantly ( $p < 0.01$ ) correlated with the EFs of the following 12 metals: Cd ( $\rho = 0.92$ ),  
185 Zn ( $\rho = 0.92$ ), Pb ( $\rho = 0.80$ ), and Ni ( $\rho = 0.80$ ) shown in Fig. 2, and Ag ( $\rho = 0.62$ ), Bi ( $\rho = 0.60$ ), Co ( $\rho = 0.50$ ), Cr ( $\rho$   
186  $= 0.60$ ), Cu ( $\rho = 0.51$ ), Mn ( $\rho = 0.63$ ), Sn ( $\rho = 0.74$ ), and Tl ( $\rho = 0.64$ ). This indicates that Factor 3 explains the EFs  
187 of the aforementioned metals. To distribute the TEs into associated groups, a cluster analysis was performed with  
188 Factors 1-3 using the Ward linkage method and the Euclidan distance measure (Fig. S4). The cluster analysis shows  
189 that Pb and Zn are strongly associated with Cd, Bi, and Mn suggesting these TEs likely have a non-crustal origin.

### 190 3.1 21st Century anthropogenic sources

191 The Mann–Kendall trend test was used to detect TEs with sustained and significant increasing trends in EF and Excess  
192 concentration during the 1971–2015 period. The trend test indicated that Bi, Cd, Ni, Pb, Tl, and Zn, which are loaded  
193 in Factor 3, have significant increasing EF trends but only Cd, Ni, Pb, and Zn have additionally significantly increasing  
194 trends in Excess concentration. The EFs obtained here using PSAs are much smaller than those calculated using the  
195 upper continental crust average (Wedepohl, 1995) and also smaller than those from ice cores with lower dust loads



196 compared to Guliya. Thus, it is necessary to determine which of the TEs mentioned above were significantly more  
197 enriched during the 2000–2015 period. For this purpose, two different tests were used, the Mann–Whitney test and  
198 the two-sample t-test ( $p < 0.0005$ ). Both tests showed that the EFs and Excess concentrations for all four metals, Cd,  
199 Zn, Pb, and Ni, are significantly higher during the 2000–2015 period than during the 1971–1990 period. Thus, the  
200 following sections will specifically focus on these TEs and their possible sources.

201 Back-trajectory frequency distributions was determined to establish the origin of air parcels reaching the Guliya ice  
202 cap. Back trajectories (7 days) were calculated daily for the 1992–2015 period for winter (December–January–  
203 February) (Fig. 1b) and summer (June–July–August) (Fig. 1c) using the HYSPLIT model from the National Oceanic  
204 and Atmospheric Administration. During winter, Guliya is strongly influenced by air parcels mostly from western  
205 Xinjiang (China); from Central Asia, which consists of the former Soviet republics of Kazakhstan, Kyrgyzstan,  
206 Tajikistan, Turkmenistan, and Uzbekistan; from Afghanistan and Pakistan in South Asia; and to a lesser extent from  
207 the Middle East, Northern Africa, Eastern, and Western Europe. In summer, westerly and southerly (monsoonal)  
208 flows, and even occasional northerly flows, influence Guliya, such that the entire Xinjiang region in addition to Central  
209 Asia and the northern regions of Afghanistan and Pakistan lies within the back trajectories area. Air parcels from other  
210 Southern Asian countries, such as India and Nepal, can also reach Guliya during summer.

211 Trace element enrichments in the Guliya core could reflect changes in emissions, atmospheric circulation, and/or post-  
212 depositional processes. Post-depositional processes (e.g., seasonal surface melting, percolation and refreezing of  
213 meltwater) do not significantly affect the stratigraphy of the Guliya core (Thompson et al., 2018). The Guliya borehole  
214 temperatures were between  $-8^{\circ}\text{C}$  and  $-12^{\circ}\text{C}$  from the surface to  $\sim 15$  m depth confirming that the ice is cold (Thompson  
215 et al., 2018) and that overprinting of the TE records due to meltwater percolation is unlikely to occur. Thus, the  
216 enrichments observed in the Guliya record indicate increasing emissions in specific source regions and/or changes in  
217 atmospheric circulation.

218 To determine the origin of the Guliya Cd, Pb, Zn, and Ni enrichments, we examine the most important emission  
219 sources of atmospheric TEs from the determined regions of influence: Central Asia, South Asia (Afghanistan,  
220 Pakistan, and India), and Xinjiang (China). We also use  $\text{PM}_{2.5}$  emission estimates, which very likely contain toxic  
221 metals such as Cd, Pb, Ni, and Zn, using the EDGAR (Emissions Database for Global Atmospheric Research) v4.3.2  
222 air pollutant dataset (1970–2012) (EDGARv4.3.2, 2017; Crippa et al., 2018). The EDGAR dataset provides total  $\text{PM}_{2.5}$   
223 and also  $\text{PM}_{2.5}$  by emission sector for all countries.

224 In the EDGAR database, the total  $\text{PM}_{2.5}$  corresponds to emissions from all human activities except large-scale biomass  
225 burning and land use, land-use change, and forestry (EDGARv4.3.2, 2017; Crippa et al., 2018). To better understand  
226 the possible emission sources, here we divided the EDGAR  $\text{PM}_{2.5}$  emission sectors into four source categories in  
227 accordance with the 2006 IPCC Guidelines for National Greenhouse Gas Inventories (IPCC, 2006). These source  
228 categories include: 1) fossil fuel combustion that comprises the emission sectors: power generation and combustion  
229 in the manufacturing, transportation, and residential sectors, 2) industrial processes which include the emission  
230 sectors: mineral, chemical, and metal industry and other production industry (note: this category does not include any  
231 type of fossil fuel combustion used by these industries), 3) agriculture which includes the emission sectors: manure



232 management, rice cultivation, direct soil emission, manure in pasture/range/paddock and other direct soil emissions,  
233 and 4) waste that includes the emission sectors: waste incineration and solid waste disposal on land.

234 From 1980 to 2012, total  $PM_{2.5}$  emissions in Afghanistan, Pakistan, India, Nepal, and China primarily originated from  
235 the fossil fuel combustion emission sectors (~80–95 %), followed by the industrial source category (~5–20 %),  
236 agriculture source category (~9 %) and waste source category (<1 % for China, no  $PM_{2.5}$  emissions estimated for waste  
237 incineration from the other countries in the EDGAR database) (EDGARv4.3.2, 2017; Crippa et al., 2018). Regarding  
238 Xinjiang in particular, numerous studies estimated coal combustion as the major source of atmospheric Cd, Pb, Zn,  
239 and Ni followed by smelting processes as a source for Cd, Pb, and Zn (Li et al., 2012; Shao et al., 2013; Cheng et al.,  
240 2014; Tian et al., 2015), and by oil combustion as a source for Ni (Tian et al., 2012). Thus, in the following sections  
241 we focus on the three largest TE and  $PM_{2.5}$  source categories: fossil fuel combustion (Sect. 3.1.1), metal production  
242 (Sect. 3.1.2), and agricultural sector (Sect. 3.1.3).

### 243 3.1.1 Fossil fuel combustion

244 In the regions that influence Guliya, two distinct trends in fossil fuel consumption and total  $PM_{2.5}$  emissions are  
245 discernible. Firstly, a steady increasing trend since the 1970s is observed in the Xinjiang province, Afghanistan,  
246 Pakistan, India, and Nepal (Fig. 4a). Secondly, a decline after the 1990s is observed in Central Asian countries due to  
247 the collapse of the Soviet Union (Fig. 4b). India and Xinjiang (China) became the largest consumers of both coal and  
248 oil in the region during the 21<sup>st</sup> century, with coal as their primary energy source (Fig. 4). The third largest consumer  
249 of coal and oil in the region during the 21<sup>st</sup> century is Kazakhstan despite its decreased consumption after the 1990s.  
250 Interestingly, for each individual country, total  $PM_{2.5}$  emissions generally follow coal consumption as shown in Fig.  
251 4.

252 Significant positive correlations were found between the Guliya EFs of Cd, Pb, Zn, and Ni and coal consumption in  
253 Xinjiang, India, China, and Pakistan; oil consumption in Xinjiang, India, China, Pakistan, and Turkmenistan; and total  
254  $PM_{2.5}$  emissions from China, India, Pakistan and Afghanistan. These positive correlations were expected since these  
255 records show generally increasing trends as shown in Fig. 4. Although Pakistan's fossil fuel consumption is 1–2 orders  
256 of magnitude lower than that of Xinjiang and India, the Guliya TE enrichments closely resemble Pakistan's coal  
257 consumption between 2005 and 2015. Both records peaked in 2008 after which they began to decrease suggesting  
258 Pakistan's coal consumption could be one of the sources of anthropogenic TEs observed in the Guliya core.

259 To further investigate the role of fossil fuel combustion in Pakistan and in the other regions, we examined  $PM_{2.5}$   
260 emitted by the different sectors comprising fossil fuel combustion. The most interesting outcome is the temporal  
261 correspondence between the Guliya TE enrichments and Pakistan's  $PM_{2.5}$  emissions from fossil fuel combustion  
262 associated with road transportation and manufacturing and construction (M-C) industries, which are the two largest  
263  $PM_{2.5}$  emission sectors in Pakistan (Fig. 5). The enrichments of Cd, Pb, Zn, and Ni have two maxima, one in 2000  
264 when  $PM_{2.5}$  emissions from road transportation peaked, and the other in 2008 when  $PM_{2.5}$  emissions from the M-C  
265 industries peaked. After 2008, TE enrichments (except for Pb) and  $PM_{2.5}$  emissions (road transportation and M-C  
266 industries) decreased (Fig. 5). These temporal similarities suggest that the TE enrichments detected in the Guliya ice



267 core after 1995 may have primarily originated from the combustion of fossil fuels in Pakistan by road transportation  
268 (since 1995) and by the M-C industries (since 2004).

269 Although Pakistan's oil and coal consumption is much lower than Xinjiang and India's, Pakistan is home to some of  
270 the most polluted cities in the world (WHO, 2016) due to the lack of emission controls and air quality standards  
271 (Colbeck et al., 2010; Sánchez-Triana et al., 2014). These cities include Peshawar, Rawalpindi, Lahore, Faisalabad,  
272 and Pakistan's capital, Islamabad (Rasheed et al., 2014; WHO, 2016; Shi et al., 2018), all located in northern Pakistan  
273 from which air parcels have been shown to strongly influence the Guliya site throughout the year. Air parcels from  
274 Xinjiang and India, on the other hand, only reach Guliya during summer (Fig. 1c) which further suggests that Pakistan  
275 is the likely dominant geographical origin of the Guliya TE enrichments.

### 276 3.1.2 Metal production

277 Like fossil fuel consumption, metal production has increased in Asia since the 1980s (Fig. S5) being China, India and  
278 Kazakhstan the most important non-ferrous metal producers in the region and in the world (BGS, 2015). In China,  
279 most of the non-ferrous metal production is located in the coastal regions while all Ni production is located in the  
280 western region of China (Gansu, Xinjiang, Chongqing, Yunnan, and Liaoning provinces). Gansu, just east of Xinjiang,  
281 produces 95 % of the total Ni production (Yanjia and Chandler, 2010). The Guliya TE enrichment trends do not  
282 resemble those of metal production in China, Pakistan, India nor Kazakhstan (Fig. S5). Thus, although these important  
283 metal production sources are relatively close to Guliya, they are likely not the primary source of the Guliya TE  
284 enrichments.

285 PM<sub>2.5</sub> emissions by industrial processes contribute ~20 %, 10 %, and 5 % to the total PM<sub>2.5</sub> emissions in Pakistan,  
286 China, and both India and Kazakhstan, respectively. Pakistan's PM<sub>2.5</sub> emissions by industrial processes peaked in  
287 2008 similar to the Guliya TE enrichments, but they remained relatively stable after that while the Guliya TE  
288 enrichments decreased (Fig. S5). Thus, while the increasing emissions from metal production could also influence the  
289 TE depositions observed in Guliya, the metal production temporal trends and the industrial PM<sub>2.5</sub> emissions suggest  
290 they are not the main sources of the Guliya TE enrichments.

### 291 3.1.3 Agricultural activities

292 Emissions from agricultural activities are an important source of atmospheric PM<sub>2.5</sub> worldwide (Lelieveld et al., 2015;  
293 Bauer et al., 2016). Fertilizers and pesticides can be a direct (aerial spreading) or indirect (soil exposed to wind erosion)  
294 source of toxic metals such as As, Cd, Cu, Cr, Pb, Ni, Zn, and others to the atmosphere (Nriagu, 1989b; Nriagu and  
295 Pacyna, 1988). In particular, fertilizers derived from phosphate rocks contain heavy metal impurities such as Cd and  
296 Pb that can contaminate agricultural soils (Mortvedt, 1995; Roberts, 2014). While consumption of phosphate fertilizers  
297 decreased in Central Asia in the 1990s, it has been increasing in China, Pakistan, India, and Nepal since the 1970s  
298 (Fig. S6). The Guliya TE enrichments do not resemble the phosphate fertilizer consumption records in these countries  
299 nor their PM<sub>2.5</sub> from agricultural activities (Fig. S6). Thus, even though agricultural activities and their emissions have



300 also been increasing since the 1970s, their depositions at the Guliya ice cap are likely overwhelmed by those from  
301 fossil fuel combustion in Pakistan.

### 302 3.2 Atmospheric circulation

303 In our previous Guliya TEs study (Sierra-Hernández et al., 2018), we observed a positive correlation between the  
304 North Atlantic Oscillation (NAO) index and the EFs at Guliya suggesting non-crustal depositions originated from  
305 regions to the west. Likewise, Thompson et al. (2018) determined possible positive linkages between NAO and the  
306 2015 Guliya ice core temperature and snowfall proxies. Fig. 6 presents a comparison of the 1992 and 2015 Guliya EF  
307 composites with the winter (DJF) NAO index and with coal production/consumption from Europe, and Pakistan  
308 between 1800 and 2015. The extended Guliya EF composite shows two periods of enrichment: ~1850–1940 and 1970–  
309 2015. We suggested that the former originated from coal consumption in Europe, which alongside the U.S. was a  
310 major coal consumer at the time. The TE enrichment dropped to pre-industrial levels during 1940–1970 coinciding  
311 with a negative NAO phase. This drop occurred at a time when atmospheric emissions in Europe reached a maximum  
312 (Pacyna and Pacyna, 2001) suggesting that atmospheric circulation (NAO) had a stronger influence over Guliya than  
313 the emission source(s) intensity. Post-1970s enrichments in both the 1992 and the 2015 Guliya records occur during  
314 positive phases of NAO. Emissions control devices were introduced in Europe ~1970 decreasing their PM<sub>2.5</sub> emissions  
315 (Pacyna et al., 2007; Pacyna and Pacyna, 2001) and consequently atmospheric emissions of TEs; however, TE  
316 enrichments continue to increase in the Guliya ice core record. This divergence can be explained by changes in either  
317 emission source intensity and/or atmospheric circulation, and indeed changes in both emission intensity and  
318 atmospheric circulation have occurred post-1990s.

319 TEs enrichments start to decrease in 2009 while the NAO entered a slightly negative phase between 2010 and 2014.  
320 Similarly, coal consumption has decreased in Pakistan since 2009, in Kazakhstan since 2012, and in Afghanistan since  
321 2011 while in Xinjiang it continues to increase. In addition, the Chinese government implemented the 12<sup>th</sup> FYP (2011–  
322 2015) that included policies to mitigate heavy metals emissions, implement air quality standards on PM<sub>2.5</sub>, and increase  
323 renewable energy consumption which likely explains the decrease of smoke and dust particles emitted in Xinjiang  
324 since 2014 (Fig. 4). The decline in coal consumption in the region, the Chinese mitigation policies and the slightly  
325 negative NAO could all have led to a decrease in EFs and Excess concentrations. However, the winter NAO index has  
326 also been slightly negative in other years (e.g., 1919, 2000) without affecting the enrichments detected in the Guliya  
327 core. Therefore, the slightly negative NAO phase between 2010 and 2014 probably did not play a significant role in  
328 the Guliya TE enrichments decrease after 2009.

329 Although practically all human activities that emit PM<sub>2.5</sub> and toxic metals have been increasing in South Asia and in  
330 Northwest China, it is very likely that emissions from Pakistan's fossil fuel combustion have dominated the Guliya  
331 Cd, Pb, Zn, and Ni enrichments during the 21<sup>st</sup> century, and more specifically oil combustion by road transportation  
332 since 1995 and the subsequent significant rise of coal combustion in 2004, likely mostly consumed by the M-C  
333 industries. Emissions from other sources (industrial processes, agriculture activities, waste disposal) from Pakistan



334 and other regions (Central Asia, Xinjiang, Afghanistan, Northwest India and Nepal) have also likely been deposited  
335 on the Guliya ice cap but to a lesser extent.

336 China is investing \$62 billion in the Pakistan-China Economic Corridor (PCEP), established in 2013, to improve the  
337 economy of Pakistan and to facilitate economic connectivity with other countries in the region. Until 2015, Pakistan's  
338 energy was generated mostly from oil, gas, and hydropower. After the establishment of the PCEP, five coal-fired  
339 power plants were built and have been operational since 2017. Three more are expected to open during 2019 and  
340 others are currently under construction (CPEC, 2019). Moving to coal-generated power will further increase the total  
341 coal consumption in Pakistan which in turn could have severe environmental and human health impacts in the region  
342 if mitigation actions are not taken.

#### 343 **4 Conclusions**

344 A new continuous, high-resolution ice core record of trace elements covering the 1971–2015 period was extracted  
345 from the Guliya ice cap in Northwestern Tibet, China. This new record extends our previous 1650–1991 Guliya record  
346 well into the 21<sup>st</sup> century making it, the first and most up to date ice core-derived archive of trace metal contamination  
347 in the Third Pole region to date. Since the dust concentrations in the Guliya ice cores are extremely high in comparison  
348 to other ice cores from the Third Pole as shown in Sierra-Hernandez et al. (2018), we also used EF and Excess  
349 concentrations to differentiate between crustal and non-crustal origins in this new record. Increases in EF and Excess  
350 concentrations of Cd, Pb, Zn, and Ni are observed since the 1990s reaching a maximum in 2008. The enrichments of  
351 Cd, Pb, Zn, and Ni increased by ~75 %, 35 %, 30 %, and 10 %, respectively during the 2000–2015 period relative to  
352 1971–1990. Comparisons between the Cd, Pb, Zn, and Ni enrichments from the Guliya records and fossil fuel  
353 consumption, metal production, phosphate fertilizer consumption, and PM<sub>2.5</sub> emissions from Xinjiang (China),  
354 Afghanistan, Pakistan, India, Nepal, and Central Asia suggest that the metal enrichments detected in Guliya originate  
355 primarily from fossil fuel combustion (road transportation and the manufacturing and construction industry) in  
356 Pakistan between 1995 and 2015. The post-2008 Cd, Zn, and Ni decline likely reflects a coal consumption decrease  
357 in Pakistan at that time. It is likely that emissions from Xinjiang, Afghanistan, India, Nepal, and Central Asia, are also  
358 impacting Guliya during the 21<sup>st</sup> century, however their contribution is overwhelmed by that of fossil fuel combustion  
359 emissions from Pakistan. This new Guliya ice core record demonstrates that the current emissions in Asia are  
360 impacting remote high-altitude glaciers in the region. Therefore, mitigation policies and technologies should be  
361 enforced by the governments of Central and South Asian countries to improve the air quality in the region as most  
362 Asian countries continue to develop.

363

364 **Data availability.**

365 **Supplement.** The Supplement is available online



366 **Author contributions.** R.S.H. wrote the paper, performed all the data analysis, interpreted the data, and ran the daily  
367 HYSPLIT back trajectories; R.S.H. and E.B. prepared the ice core samples and conducted their ICP-MS analysis; E.B.  
368 created the maps for Fig. 1. All authors contributed to the study design, data interpretation, revision and edition of the  
369 manuscript. P.G. oversees the ICP-MS lab. L.G.T. planned the drilling operation and led the field expedition in which  
370 both L.G.T. and P.G. contributed to the ice core processing in the field.

371 **Competing interests.** The authors declare no competing financial interests.

### 372 **Acknowledgments**

373 The NSF P2C2 program (1502919) funded this study. We thank everybody that made the 2015 Guliya field expedition  
374 a success, in particular Tandong Yao from the Institute for Tibetan Plateau Research. The authors greatly acknowledge  
375 Julien Nicolas for creating the seasonal back trajectory frequencies grid for all our Guliya TEs publications as well as  
376 for his time discussing them. We thank Aaron Wilson for his insights on the meteorology of the region. We thank  
377 Xiaoxing Yang and Chao You for providing recent energy yearbook data from Xinjiang. We also thank Max  
378 Woodworth for helpful discussions about the development and policies in Western China. We are grateful to Ellen  
379 Mosley-Thompson and Mary Davis for valuable comments throughout the development of the manuscript. Stacy  
380 Porter is greatly acknowledged for her help in editing and improving the English of the different versions of the  
381 manuscript. Lastly, we thank Henry Brecher for his detailed proofreading of the manuscript.

### 382 **References**

- 383 Bajwa, A., Compendium of Environmental Statistics of Pakistan. Pakistan Bureau of Statistics. 258, 2015.
- 384 Bauer, S. E., Tsigaridis, K., and Miller, R.: Significant atmospheric aerosol pollution caused by world food cultivation,  
385 *Geophys. Res. Lett.*, 43, 5394-5400, 10.1002/2016gl068354, 2016.
- 386 Beaudon, E., Gabrielli, P., Sierra-Hernández, M. R., Wegner, A., and Thompson, L. G.: Central Tibetan Plateau  
387 atmospheric trace metals contamination: A 500-year record from the Puruogangri ice core, *Sci. Total Environ.*, 601-  
388 602, 1349-1363, 2017.
- 389 BGS, British Geological Survey. World Mineral Statistics and World Mineral Production, 2/1/2018, 2015.
- 390 BP, British Petroleum (BP) Statistical Review of World Energy, 6/20/2016, 9/20/2016, 2016.
- 391 Chen, W., Li, H., and Wu, Z.: Western China energy development and west to east energy transfer: Application of the  
392 Western China Sustainable Energy Development Model, *Energy Policy*, 38, 7106-7120, 2010.
- 393 Cheng, K., Tian, H. Z., Zhao, D., Lu, L., Wang, Y., Chen, J., Liu, X. G., Jia, W. X., and Huang, Z.: Atmospheric  
394 emission inventory of cadmium from anthropogenic sources, *Int. J. Environ. Sci. Technol.*, 11, 605-616,  
395 10.1007/s13762-013-0206-3, 2014.



- 396 Colbeck, I., Nasir, Z. A., and Ali, Z.: The state of ambient air quality in Pakistan—a review, *Environ. Sci. Pollut. R.*,  
397 17, 49-63, 10.1007/s11356-009-0217-2, 2010.
- 398 Cooke, C. A., and Bindler, R.: Lake Sediment Records of Preindustrial Metal Pollution, in: *Environmental*  
399 *Contaminants. Developments in Paleoenvironmental Research*, edited by: Blais, J., Rosen, M., and Smol, J., Springer,  
400 Dordrecht, 101-119, 2015.
- 401 China Pakistan Economic Corridor: <http://cpec.gov.pk/>, access: 4 April 2019, 2019.
- 402 Crippa, M., Guizzardi, D., Muntean, M., Schaaf, E., Dentener, F., van Aardenne, J. A., Monni, S., Doering, U., Olivier,  
403 J. G. J., Pagliari, V., and Janssens-Maenhout, G.: Gridded emissions of air pollutants for the period 1970–2012 within  
404 EDGAR v4.3.2, *Earth Syst. Sci. Data*, 10, 1987-2013, 10.5194/essd-10-1987-2018, 2018.
- 405 Dong, W., and Yang, Y.: Exploitation of mineral resource and its influence on regional development and urban  
406 evolution in Xinjiang, China, *J. Geog. Sc.*, 24, 1131-1146, 10.1007/s11442-014-1143-x, 2014.
- 407 EDGARv4.3.2, European Commission, Joint Research Centre (EC-JRC)/Netherlands Environmental Assessment  
408 Agency (PBL). Emissions Database for Global Atmospheric Research (EDGAR), release EDGAR v4.3.2 (1970 -  
409 2012), 2017.
- 410 EIA, U.S. Energy Information Administration, 2/28/2019, 2019.
- 411 Fridley, D., Lu, H., and Liu, X.: *China Energy Databook 9.0*, 9th ed., edited by: Group, C. E., Lawrence Berkeley  
412 National Laboratory, United States, 2017.
- 413 Gabrielli, P., and Vallelonga, P.: Contaminant Records in Ice Cores, in: *Environmental Contaminants. Developments*  
414 *in Paleoenvironmental Research*, edited by: Blais, J., Rosen, M., and Smol, J., Springer, Dordrecht, 393-430, 2015.
- 415 Hansson, S., Bindler, R., and De Vleeschouwer, F.: Using Peat Records as Natural Archives of Past Atmospheric  
416 Metal Deposition, in: *Environmental Contaminants. Developments in Paleoenvironmental Research*, edited by: Blais,  
417 J., Rosen, M., and Smol, J., Springer, Dordrecht, 323-354, 2015.
- 418 IPCC: 2006 IPCC Guidelines for National Greenhouse Gas Inventories, in, edited by: Eggleston, S., Buendia, L.,  
419 Miwa, K., Ngara, T., and Tanabe, K., Hayama, Japan, 2006.
- 420 Lai, H. H.: China's Western Development Program: Its Rationale, Implementation, and Prospects, *Modern China*, 28,  
421 432-466, 2002.
- 422 Lelieveld, J., Evans, J. S., Fnais, M., Giannadaki, D., and Pozzer, A.: The contribution of outdoor air pollution sources  
423 to premature mortality on a global scale, *Nature*, 525, 367-371, 10.1038/nature15371, 2015.



- 424 Li, Q., Cheng, H., Zhou, T., Lin, C., and Guo, S.: The estimated atmospheric lead emissions in China, 1990-2009,  
425 Atmos. Environ., 60, 1-8, 2012.
- 426 Liu, F., Zhang, Q., Tong, D., Zheng, B., Li, M., Huo, H., and He, K. B.: High-resolution inventory of technologies,  
427 activities, and emissions of coal-fired power plants in China from 1990 to 2010, Atmos. Chem. Phys., 15, 13299-  
428 13317, 10.5194/acp-15-13299-2015, 2015.
- 429 Marx, S. K., and McGowan, H. A.: Long-Distance Transport of Urban and Industrial Metals and Their Incorporation  
430 into the Environment: Sources, Transport Pathways and Historical Trends, in: Urban Airborne Particulate Matter.  
431 Origin, Chemistry, Fate and Health Impacts, edited by: Zereini, F., and Wiseman, C. L. S., Springer, Berlin, 103-123,  
432 2010.
- 433 Marx, S. K., Rashid, S., and Stromsoe, N.: Global-scale patterns in anthropogenic Pb contamination reconstructed  
434 from natural archives, Environ. Pollut., 213, 283-298, 2016.
- 435 Moore, J. C., and Grinsted, A.: Ion Fractionation and Percolation in Ice Cores with Seasonal Melting, Physics of Ice  
436 Core Records II, Suppl Issue of Low Temperature Science, 68, 287-298, 2009.
- 437 Mortvedt, J. J.: Heavy metal contaminants in inorganic and organic fertilizers, Fertilizer Res., 43, 55-61,  
438 10.1007/bf00747683, 1995.
- 439 Ning, J.: China Statistical Yearbook, 2016.
- 440 Nriagu, J. O., and Pacyna, J. M.: Quantitative assessment of worldwide contamination of air, water and soils by trace  
441 metals, Nature, 333, 134-139, 1988.
- 442 Nriagu, J. O.: Natural Versus Anthropogenic Emissions of Trace Metals to the Atmosphere, in: Control and Fate of  
443 Atmospheric Trace Metals, edited by: Pacyna, J., and Ottar, B., Mathematical and Physical Sciences, 268, Kluwer  
444 Academic Publishers, 3-13, 1989a.
- 445 Nriagu, J. O.: A global assessment of natural sources of atmospheric trace metals, Lett. Nature, 338, 47-49, 1989b.
- 446 Pacyna, E. G., Pacyna, J. M., Fudala, J., Strzelecka-Jastrzab, E., Hlawiczka, S., Panasiuk, D., Nitter, S., Pregger, T.,  
447 Pfeiffer, H., and Friedrich, R.: Current and future emissions of selected heavy metals to the atmosphere from  
448 anthropogenic sources in Europe, Atmos. Environ., 41, 8557-8566, 2007.
- 449 Pacyna, J. M., and Pacyna, E. G.: An assessment of global and regional emissions of trace metals to the atmosphere  
450 from anthropogenic sources worldwide, Environ. Rev., 9, 269-298, 2001.



- 451 Rasheed, A., Aneja, V. P., Aiyyer, A., and Rafique, U.: Measurements and analysis of air quality in Islamabad,  
452 Pakistan, *Earth's Future*, 2, 303-314, 10.1002/2013ef000174, 2014.
- 453 Roberts, T. L.: Cadmium and Phosphorous Fertilizers: The Issues and the Science, *Procedia Eng.*, 83, 52-59,  
454 <https://doi.org/10.1016/j.proeng.2014.09.012>, 2014.
- 455 Rolph, G., Stein, A., and Stunder, B.: Real-time Environmental Applications and Display sYstem: READY, *Environ.*  
456 *Model. Softw.*, 95, 210-228, 2017.
- 457 Sánchez-Triana, E., Enriquez, S., Afzal, J., and Nakawaga, A.: Air Pollution in Pakistan, in: *Cleaning Pakistan's Air:*  
458 *Policy Options to Address the Cost of Outdoor Air Pollution*, 57-81, 2014.
- 459 Shao, X., Cheng, H., Li, Q., and Lin, C.: Anthropogenic atmospheric emissions of cadmium in China, *Atmos.*  
460 *Environ.*, 79, 155-160, 2013.
- 461 Shi, Y., Matsunaga, T., Yamaguchi, Y., Li, Z., Gu, X., and Chen, X.: Long-term trends and spatial patterns of satellite-  
462 retrieved PM<sub>2.5</sub> concentrations in South and Southeast Asia from 1999 to 2014, *Sci. Total Environ.*, 615, 177-186,  
463 <https://doi.org/10.1016/j.scitotenv.2017.09.241>, 2018.
- 464 Sierra-Hernández, M. R., Gabrielli, P., Beaudon, E., Wegner, A., and Thompson, L. G.: Atmospheric depositions of  
465 natural and anthropogenic trace elements on the Guliya ice cap (northwestern Tibetan Plateau) during the last 340  
466 years, *Atmos. Environ.*, 176, 91-102, 2018.
- 467 Stein, A. F., Draxler, R. R., Rolph, G. D., Stunder, B. J. B., Cohen, M. D., and Ngan, F.: NOAA's HYSPLIT  
468 Atmospheric Transport and Dispersion Modeling System, *Bull. Am. Meteorol. Soc.*, 96, 2059-2077, 10.1175/bams-  
469 d-14-00110.1, 2015.
- 470 Thompson, L. G., Mosley-Thompson, E., Davis, M. E., Lin, P.-N., Mikhailenko, V., and Dai, J.: A 1000 year ice core  
471 climate record from the Guliya Ice Cap, China and its relationship to global climate variability, *Ann. Glaciol.*, 21,  
472 175-181, 1995.
- 473 Thompson, L. G., Yao, T., Davis, M. E., Mosley-Thompson, E., Wu, G., Porter, S. E., Xu, B., Lin, P.-N., Wang, N.,  
474 Beaudon, E., Duan, K., Sierra-Hernández, M. R., and Kenny, D. V.: Ice core records of climate variability on the  
475 Third Pole with emphasis on the Guliya ice cap, western Kunlun Mountains, *Quat. Sci. Rev.*, 188, 1-14, 2018.
- 476 Tian, H. Z., Lu, L., Cheng, K., Hao, J. M., Zhao, D., Wang, Y., Jia, W. X., and Qiu, P. P.: Anthropogenic atmospheric  
477 nickel emissions and its distribution characteristics in China, *Sci. Total Environ.*, 417-418, 148-157,  
478 <https://doi.org/10.1016/j.scitotenv.2011.11.069>, 2012.



479 Tian, H. Z., Zhu, C. Y., Gao, J. J., Cheng, K., Hao, J. M., Wang, K., Hua, S. B., Wang, Y., and Zhou, J. R.: Quantitative  
480 assessment of atmospheric emissions of toxic heavy metals from anthropogenic sources in China: historical trend,  
481 spatial distribution, uncertainties, and control policies, *Atmos. Chem. Phys.*, 15, 10127-10147, 2015.

482 Uglietti, C., Gabrielli, P., Olesik, J. W., Lutton, A., and Thompson, L. G.: Large variability of trace element mass  
483 fractions determined by ICP-SFMS in ice core samples from worldwide high altitude glaciers, *Appl. Geochem.*, 47,  
484 109-121, 2014.

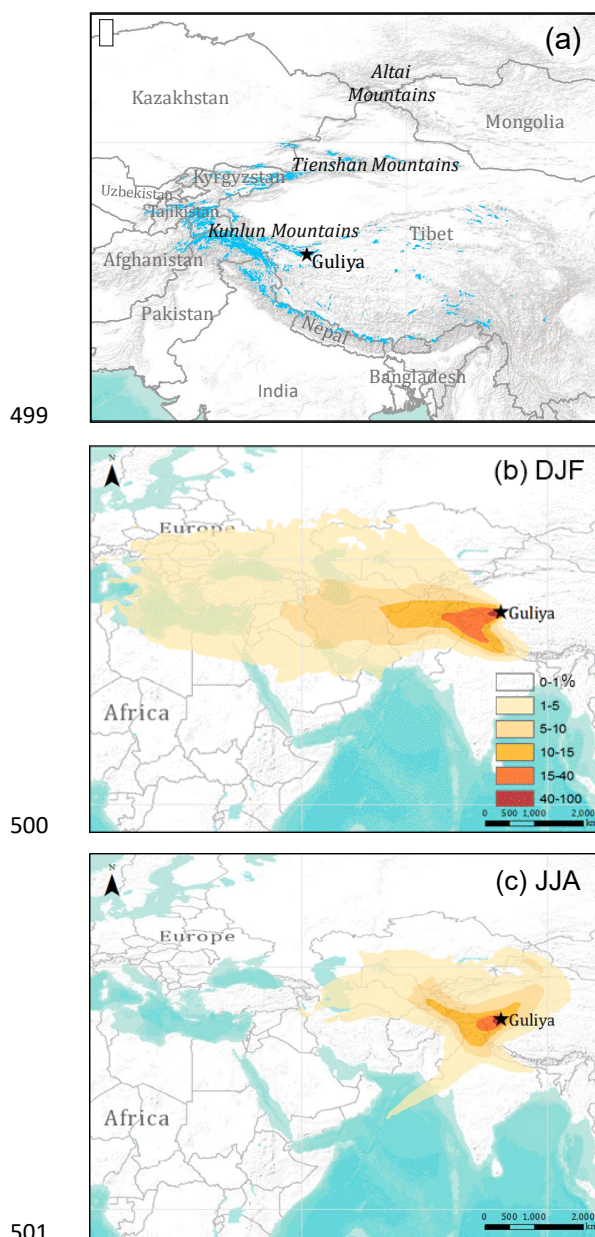
485 UN, United Nations. Department of Economic and Social Affairs, Population Division. *World Population Prospects:  
486 The 2017 Revision*, 2017.

487 Wedepohl, K. H.: The composition of the continental crust, *Geochim. Cosmochim. Acta*, 59, 1217-1232, 1995.

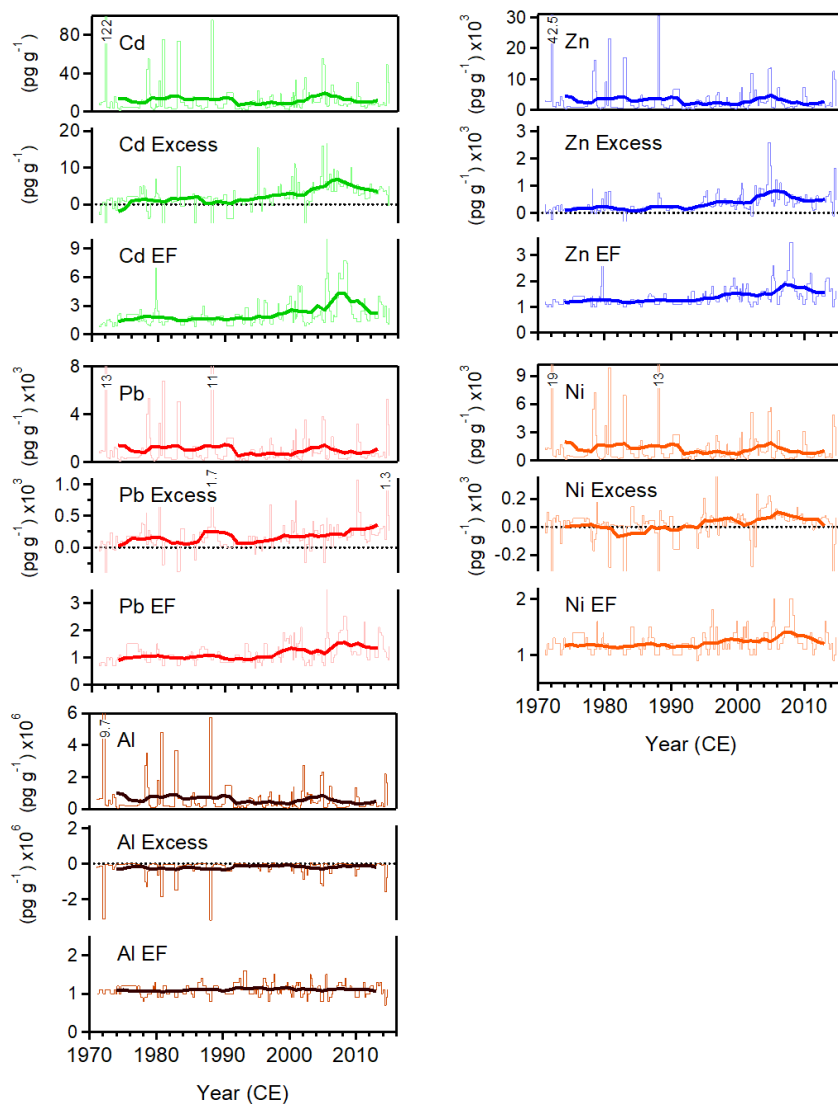
488 WHO, World Health Organization. *Ambient Air Pollution Database*, 2016.

489 Yanjia, W., and Chandler, W.: The Chinese nonferrous metals industry—energy use and CO<sub>2</sub> emissions, *Energy  
490 Policy*, 38, 6475-6484, 10.1016/j.enpol.2009.03.054, 2010.

491  
492  
493  
494  
495  
496  
497  
498



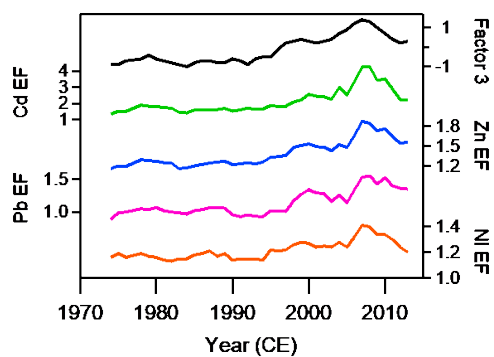
502 **Figure 1.** Maps showing the location of the Guliya ice cap (star) and the three mountain ranges of the Xinjiang  
503 province (a), and seasonal NOAA HYSPLIT 7-day back trajectories frequency plots for December, January, and  
504 February (b); and June, July, and August (c) for the 1992–2015 period (Rolph et al., 2017; Stein et al., 2015).



505

506 **Figure 2.** Cd, Pb, Zn, Ni, and Al 5-year running means (thick lines) of concentrations and EFs between 1971 and  
507 2015. Thin lines show the sample resolution.

508



509

510 **Figure 3.** Comparison of 5-year running means of Factor 3 scores with Cd, Zn, Pb and Ni EFs between 1971 and  
511 2015.

512

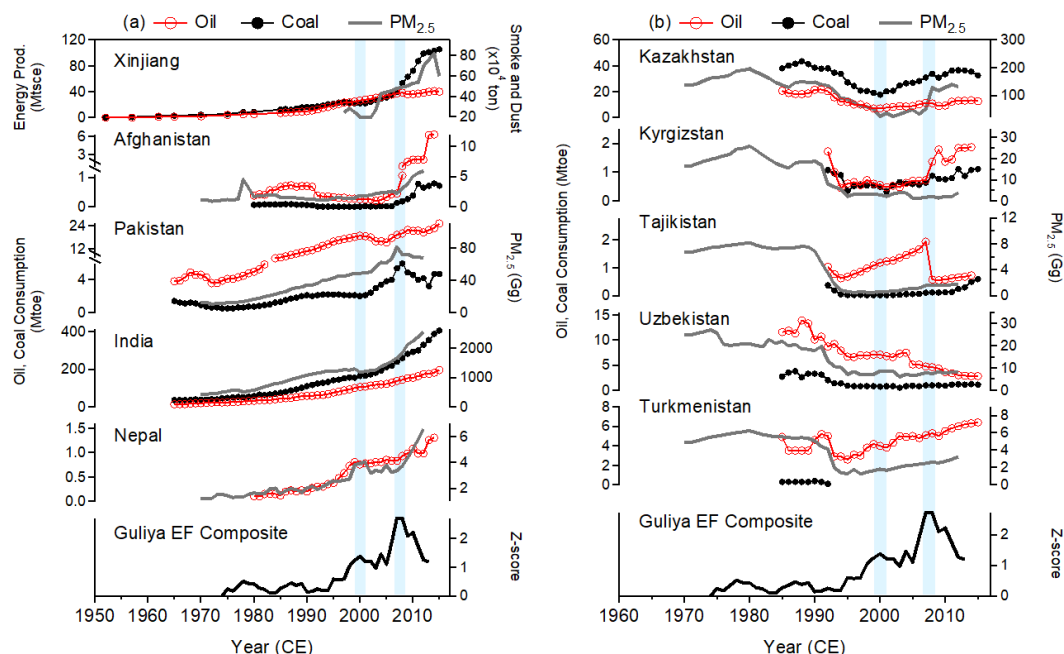
513

514

515

516

517

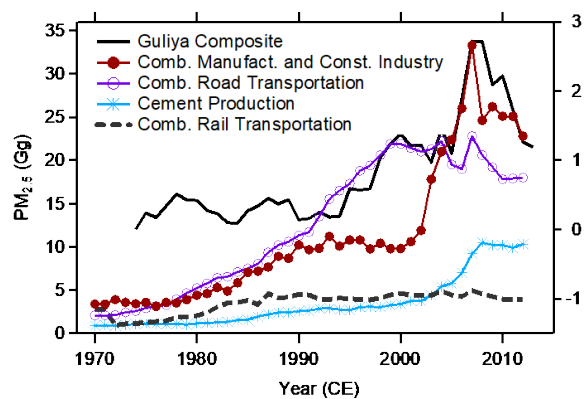


518

519 **Figure 4.** Oil and coal consumption in: (a) Xinjiang, as coal energy production in million tonnes of standard coal  
 520 equivalent (Jianxin, 2016); in million tonnes of oil equivalent (Mtoe) in Afghanistan (EIA, 2019), Pakistan (BP,  
 521 2016), India (BP, 2016), and Nepal (coal  $\leq 0.1$  Mtoe) (EIA, 2019). (b) Central Asian countries: Kazakhstan (BP,  
 522 2016), Kyrgyzstan and Tajikistan (EIA, 2019), and Uzbekistan and Turkmenistan (BP, 2016).  $PM_{2.5}$  emissions from  
 523 anthropogenic sources (EDGARv4.3.2, 2017; Crippa et al., 2018) shown in both panels for all countries except  
 524 Xinjiang (China). Smoke and dust emissions from Xinjiang (China) (Ning, 2016) are shown since no  $PM_{2.5}$  data was  
 525 available. The Guliya EF composite (average of Cd, Pb, Zn, and Ni EF z-scores) is shown at the bottom of each  
 526 panel for comparison. The two Guliya maxima at 2000 and 2008 are shown as shaded bars.

527

528



529

530 **Figure 5.** Largest emitter sectors of  $PM_{2.5}$  in Pakistan between 1970 and 2012: fossil fuel combustion in  
531 manufacturing and construction industries, fossil fuel combustion by road transportation, cement production, and  
532 fossil fuel combustion by rail transportation (EDGARv4.3.2, 2017; Crippa et al., 2018). The Guliya EF composite  
533 (average of Cd, Pb, Zn, and Ni EF z-scores) is shown for comparison.

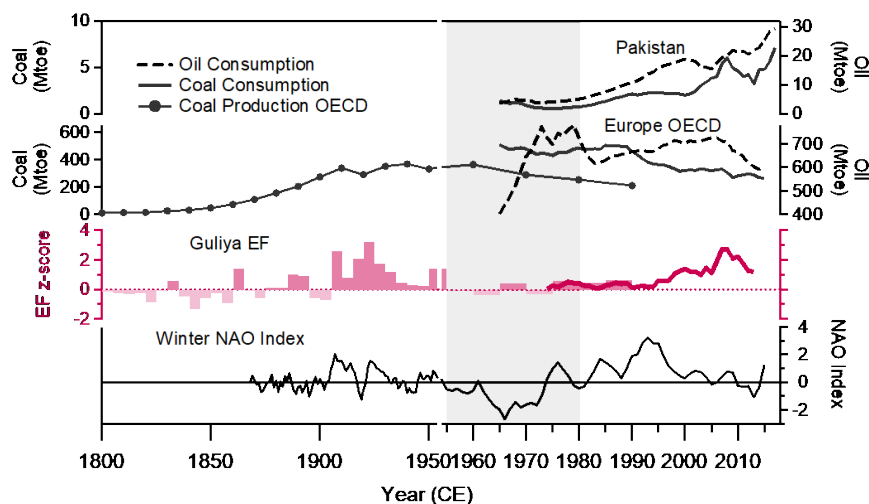
534

535

536

537

538



539

540 **Figure 6.** Comparisons of the Guliya EF composite (average of Cd, Pb, Zn, and Ni EF z-scores) from the 2015  
541 Guliya core with the winter NAO index shown as 5-year running mean (Hurrell, 2003). The 1992 Guliya EF  
542 composite (average of Cd, Pb, and Zn EF z-scores) is shown as 5-year medians and the 2015 Guliya EF composite is  
543 a 5-year running mean. The light gray band (1955–1980) highlights the period of negative NAO. Pakistan’s and  
544 Europe coal and oil consumption (1965–2017) (BP, 2016) are shown for comparison. Europe’s coal production  
545 (1800–1990) (HYDE, 2006) is also shown. Mtoe is million tonnes of oil equivalent.

546

547